Crystal Structure of Fragment D from Lamprey Fibrinogen Complexed with the Peptide Gly-His-Arg-Pro-amide[†,‡]

Zhe Yang, Glen Spraggon,[§] Leela Pandi, Stephen J. Everse,[||] Marcia Riley, and Russell F. Doolittle*

Center for Molecular Genetics, University of California, San Diego, La Jolla, California 92093-0634

Received April 23, 2002

ABSTRACT: The crystal structure of fragment D from lamprey fibrinogen has been determined at 2.8 Å resolution. The 89 kDa protein was cocrystallized with the peptide Gly-His-Arg-Pro-amide, which in many fibrinogens—but not lamprey—corresponds to the B knob exposed by thrombin. Because lamprey fragment D is more than 50% identical in sequence with human fragment D, the structure of which has been reported previously, it was possible to use the method of molecular replacement. The space group of the lamprey crystals is *P*1; there are four molecules in the unit cell. Although the fragments are packed head to head by the same D:D interface as is observed in other related preparations containing fragments D, the tails are uniquely joined by an unnatural association of the terminal sections of the residual coiled coils from adjacent molecules. Some features of the lamprey structure are clearer than have been observed in previous fragment D structures, including the β-chain carbohydrate cluster, for one, and the important γ-chain carboxyl-terminal segment, for another. The most significant differences between the lamprey and human structures occur in connecting loops at the entryways to the β-chain and γ-chain binding pockets.

Lampreys and hagfish comprise the earliest diverging group of vertebrate animals; they are also the most primitive creatures known to have a thrombin-clottable fibrinogen (*1*, *2*). The lamprey protein has the same subunit composition as all other vertebrate fibrinogens ($\alpha_2\beta_2\gamma_2$). In this regard, the β and γ chains are both about 50% identical with their mammalian counterparts, but the α chains are more distinctive, having experienced a relatively recent series of internal duplications that gave rise to 25 18-residue repeats in the regions tethering their carboxyl domains to the main framework of the molecule (*3*).

Lamprey fibrinogen can be clotted with mammalian thrombins, but in the process only the fibrinopeptide B is released (*2*, *4*). The new amino-terminal segment exposed by the cleavage has the sequence Gly-Val-Arg, different from the Gly-His-Arg that occurs in all known mammalian fibrinogen "B knobs". On the other hand, lamprey thrombin releases both the fibrinopeptides A and B, the "A knob" having the absolutely conserved sequence Gly-Pro-Arg that occurs in all known vertebrate fibrinogens.

Synthetic knobs beginning with the sequence Gly-Pro-Arg severely inhibit fibrin formation in lamprey no matter which thrombin is employed. Peptides beginning with Gly-Val-Arg (the lamprey B knob) have only a slight effect, and Gly-His-Arg peptides do not inhibit fibrin formation at all, even though they bind to lamprey fibrinogen (*5*). These apparently contradictory observations make it clear that we do not yet have a full understanding of the role of the B knobs in fibrin formation. In an effort to untangle these events, we have determined the structure of lamprey fibrinogen fragment D complexed with the synthetic peptide GHRPam.[1] Comparisons with the equivalent human fragment D complex have revealed both obvious similarities and subtle differences.

MATERIALS AND METHODS

Lamprey fibrinogen was prepared by a modified cold ethanol procedure (*6*) and was digested with human plasmin (Kabi) for 4 h at room temperature, after which an appropriate amount of aprotinin (Trasylol) was added to stop the reaction. Fragment D was obtained by affinity chromatography of the digest on a Gly-Pro-Arg-Pro affinity column (*7*, *8*). The pooled peak fractions were concentrated by the addition of one-third volume of saturated ammonium sulfate; the precipitate was dissolved in a minimal volume of 0.05 M Tris, pH 7.0, and 5 mM $CaCl_2$ and dialyzed against the same buffer to remove ammonium sulfate. Protein solutions (8−10 mg/mL) were stored at −70 °C.

Crystals were grown by vapor diffusion from sitting drops at room temperature. PEG-3350 was used as a precipitant. Solutions containing 6−8 mg/mL lamprey fragment D, 50 mM Tris, pH 7.0, 4 mM GHRPam, and 5 mM $CaCl_2$ were combined with an equal volume of 12% PEG and 50 mM MES buffer, pH 6.5, containing 20 mM $CaCl_2$. The lower

[†] This work was supported by Grant HL-26873 from the National Heart, Lung, and Blood Institute.

[‡] Atomic coordinates are available from the Protein Data Bank under the access code 1LWU.

* Corresponding author. Tel: (858) 534-4417. Fax: (858) 534-4985. E-mail: rdoolittle@ucsd.edu.

[§] Present address: Novartis Institute of Functional Genomics, La Jolla, CA.

[||] Present address: Department of Biochemistry, University of Vermont, Burlington, VT.

[1] Abbreviations: GPRPam, Gly-Pro-Arg-Pro-amide; GHRPam, Gly-His-Arg-Pro-amide; GPRP, Gly-Pro-Arg-Pro; GVRP, Gly-Val-Arg-Pro; t-PA, tissue plasminogen activator.

10.1021/bi020299t CCC: $22.00 © 2002 American Chemical Society
Published on Web 07/12/2002

Table 1: Data Collection and Refinement Statistics

space group	*P*1
unit cell dimensions (Å/deg)	$a = 76.74$, $b = 47.65$, $c = 244.65$ $\alpha = 88.8$, $\beta = 97.2$, $\gamma = 86.2$
molecules/asym unit	4
no. of crystals	1
highest resolution (Å)	2.80
observations (*N*)	200629
unique reflections (*N*)	74102
completeness (%)	88.3
completeness in highest shell (2.87−2.80 Å) (%)	58.4
R_{sym} (*I*) (%)[a]	0.078
mosaicity	0.55
refinement resoln range (Å)	20.0−2.8
no. of residues in protein	765
no. of residues in model	733 (96%)
R-value[b]	0.241
free *R*-value[c]	0.289
rmsd from ideals	
bond length (Å)	0.008
bond angle (deg)	1.38

[a] $R_{sym} = (\Sigma|I - \langle I\rangle|)/(\Sigma|I|)$. [b] Crystallographic *R*-value $[(\Sigma||F_o| - |F_c||)/(\Sigma|F_o|)]$ with 95% of the native data for refinement. [c] Free *R*-value: *R*-value based on 5% of the native data withheld from refinement.

pH at which crystallization occurs relative to human fragment D is likely a reflection of its lower isoelectric point, the lamprey D having more negatively charged side chains and fewer positively charged ones than its human counterpart.

Diffraction data were collected at the National Light Source, Brookhaven National Laboratory, beamline X-12C. Although data were collected from numerous crystals, only data from a single frozen specimen (20% glycerol as a cryoprotectant) were used for the structure determination. Data were processed with DENZO and Scalepack (*9*). Molecular replacement was carried out with AMORE (*10*). Extensive use was made of various programs in the CCP4 package (*11*). Model building was conducted with O (*12*) and refinement with cns (*13*); the free *R*-factor (*14*) was used as a guide throughout. Illustrations were prepared with various software programs (*15*−*18*).

Residue Numbering. Residue numbering for the various vertebrate fibrinogens is most affected by the great variability in the lengths of the fibrinopeptides A and B. Lamprey fibrinogen represents an extreme case, having the shortest known fibrinopeptide A (only 6 residues) and one of the longest fibrinopeptides B (36 residues). Because certain residues in the human structure are well-known for their functional importance, we have mostly employed human numbering (*19*), except in a few cases where the lamprey numbering is more appropriate and is specified as such.

RESULTS

Molecular Replacement. A rotation search using one fragment D unit from a human double-D structure (*20*) as a search model yielded four solutions when the data from 10 to 4 Å were used, consistent with there being four molecules in the unit cell of the *P*1 space group. When these top solutions were considered together, the correlation coefficient was 33.1 and the *R*-factor 48.6. From this point on, all data between 20 and 2.8 Å were used. SigmaA-weighted electron density maps were constructed (*21*), including $|2F_o - F_c|$, $|3F_o - 2F_c|$, and $|F_o - F_c|$ maps. Numerous cycles of rebuilding and refinement were conducted. NCS restraints were kept in place for all four βC and γC domains throughout the procedure. In the end, the working *R*-factor was 0.241 and the free *R*-factor 0.289 (Table 1).

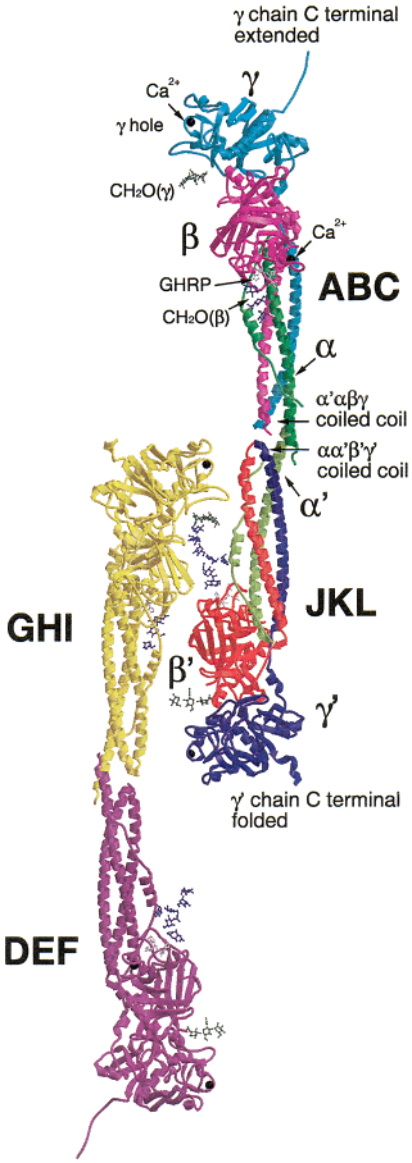

FIGURE 1: Cα backbone structures of four molecules in the unit cell of lamprey fragment D. The structures have been depicted in a way to emphasize intermolecular contacts; note especially the artifactual coiled coil between the amino-terminal segments. Also note the two different conformations for γ-chain carboxyl-terminal segments.

Crystal Packing. Even though the same end-to-end packing occurs in the lamprey fragment D crystals as has been observed in all previous fragment D or double-D preparations, the overall packing is very different. Instead of there being a close side-by-side packing of γ-chain carboxyl domains, the major lateral contacts involve extended loops from the β-carboxyl domain. In one of these the contact is between the loop composed of residues β357−β360 on the E and K molecules and another made up of residues β316−β320 on the B and H molecules, respectively (human numbering). Another contact involves the asparaginyl-linked carbohydrate cluster at β364 (E and K molecules, human numbering) and the loop composed of β242−β247 on the adjacent molecules (B and H) (Figure 1).

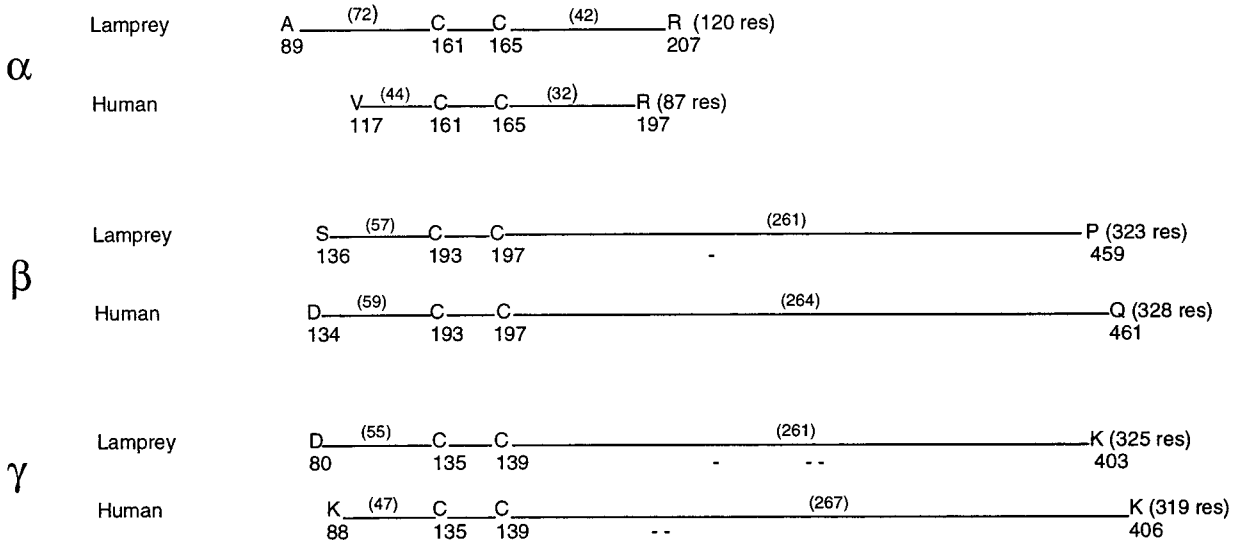

FIGURE 2: Diagrammatic depiction of the three chains in lamprey and human fragments D. The differences in chain length reflect different susceptible targets for human plasmin. Numbers in parentheses denote numbers of residues extending on either side of the disulfide rings. Dashes indicate small gaps in aligned sequences.

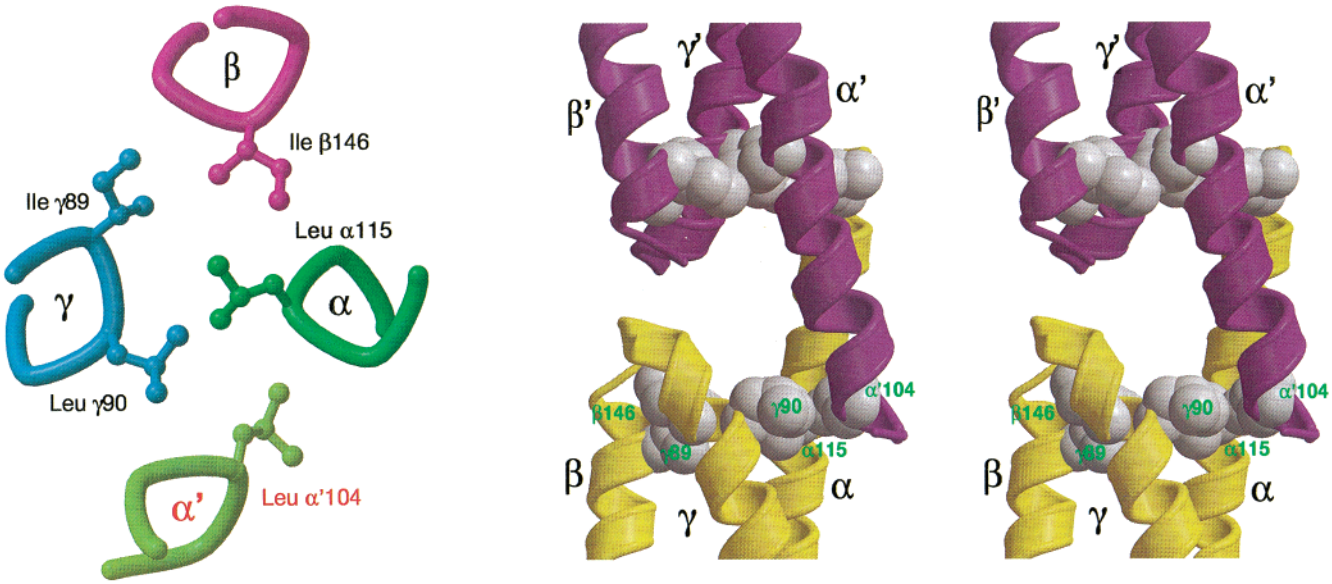

FIGURE 3: Close-up views of the hydrophobic interaction involved in the association of coiled coils in crystals of lamprey fragment D. (Left) Diagrammatic section through the hydrophobic cluster involving four chains. (Right) Stereo projection of the same hydrophobic cluster.

The most intriguing interaction occurs between the residual coiled coils of adjacent molecules near their amino terminals. The major contributants are from the α-chains, the terminal segments of which—as a happenstance of susceptibility to cleavage by human plasmin—are longer than their β- and γ-chain counterparts (Figure 2). During the crystallization the α chains have formed an antiparallel fourth component to the native three-stranded coiled coil; at one key nexus hydrophobic side chains from all three chains of the coiled coil interact with each other and the α chain from the other molecule (Figure 3).

Because of differences in the crystal packing for the different molecules in the unit cell, the electron density for each had regions that were clearer, or not so clear, relative to the others. Actually, the four molecules fall, more or less, into two sets of two; in molecules ABC and DEF it was possible to build the γ-chain carboxyl-terminal segment out to the glutamine residue at γ399 (lamprey numbering), whereas in molecules GHI and JKL the discernible density disappeared at residue Glyγ395 (lamprey numbering). Similarly, the carbohydrate at Asnβ364 (human numbering; lamprey Asnβ384) was exceptionally clear in molecules JKL and DEF, where it was possible to build seven sugar residues into the density.

Main Structural Features. The overall structure of lamprey fragment D is similar to that of the corresponding fragment from human fibrinogen complexed with GHRPam (Figure 4). Comparison of the individual βC and γC domains was more revealing, however, important loops being significantly different in both instances. Thus, residues γ357−γ361, which constitute one side of the γ-chain binding pocket, are situated very differently in the human and lamprey structures (Figure 5, left). In the case of the β-chain hole, it is the loop made up of β386−β392, on one of the other sides of the pocket, that differs (Figure 5, right). Remarkably, in both pockets the residues directly involved in binding the ligands are

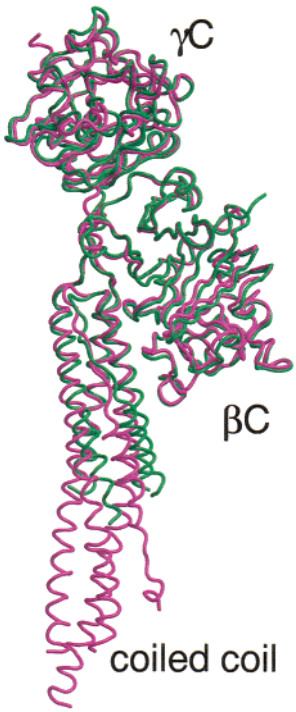

FIGURE 4: Superposition of Cα backbone traces from lamprey (red) and human (green) fragments D complexed with GHRPam (the human structure PDB code is 1FZG). The least-squares operation in O (*13*) was based on the most conserved regions of the *β*C and *γ*C domains.

positioned in exactly the same way in the lamprey and human proteins, even though the entryway loops differ significantly.

All told, there are four small gaps (one or two residues each) in the alignment of the lamprey and human sequences (Figure 2). All are in connecting loops and at sites where there are also gaps in an alignment of the homologous *β* and *γ* chains. For example, the single one-residue gap in the *β* chain occurs in the region previously designated "the snout" (*23*), an eight-residue insert (*β*280−*β*287, human numbering) in the *β* chain relative to the *γ* chain.

In another case, a short helix takes the place of a simple extended strand as the result of two extra residues in the lamprey *γ* chain (residues 144A and 144B, human numbering). Similarly, the lamprey *γ* chain lacks human residues 242 and 243, an extended loop merely being truncated.

Peptide Binding. The GHRPam ligand was clearly evident in the *β*-chain binding site (Figure 6). As expected, the side chains of Glu*β*397 and Asp*β*398 are key interactants in binding to the positively charged α-amino and arginyl guanidino groups in the ligand. The peptide was not observed in the *γ*-chain hole, although the electron density in this region was relatively diffuse.

The D:D Interface. As noted above, the D:D interface that occurs naturally during fibrin formation invariably contributes to the crystal packing of fragments D and double-D (*20*, *22*, *23*), as well as in crystals of a modified bovine fibrinogen (*24*) and native chicken fibrinogen (*25*). The interface is asymmetric, the two participating molecules being arbitrarily assigned as A or B on the basis of the residues they contribute (*23*). In the human system, the A molecule is defined as the one that has Arg*γ*275 interacting with Tyr*γ*280 of its B partner, the latter having its Arg*γ*275 interacting with Ser*γ*300 from A. As it happens, although Arg*γ*275 is conserved in the lamprey, both of the opposing residues are changed, without apparent consequence. Indeed, the complementarity of the interface looks to be highly conserved despite a number of amino acid replacements (Figure 7). As in past structures, the interface is virtually devoid of obvious intermolecular interactions. One possible new exception is a putative hydrophobic interaction between Met*γ*280 of the A molecule and Phe*γ*277 of the B molecule.

In a previous report comparing human fragments D (and double-D), a perceptible difference was observed in the orientation of the A and B molecules in the double-D fragment complexed with GHRPam, relative to other complexes, the crevice being wider on one side than occurs when GPRPam is present or when there is no ligand at all (*22*). The lamprey fragment D−GHRPam complex, while maintaining the same general arrangement, appears to fall in an intermediate position between the two kinds of human complex (data not shown).

γ-Chain Carboxyl-Terminal Segment. The lamprey fragment D provides a clearer picture of the *γ*-chain carboxyl region than any of the several human fragments D previously reported (*22*, *23*). Two different conformations are present: an extended form arising on one side of the D:D interface and a bent or folded form on the other side (Figure 1). The extended form could be traced as far as Gln*γ*399 (lamprey numbering, *γ*401 human numbering); the density for the bent form faded after residue Gly*γ*395 (lamprey numbering, *γ*397 human numbering). It should be noted that in lamprey fibrinogen the putative cross-link acceptor sites (glutamines)

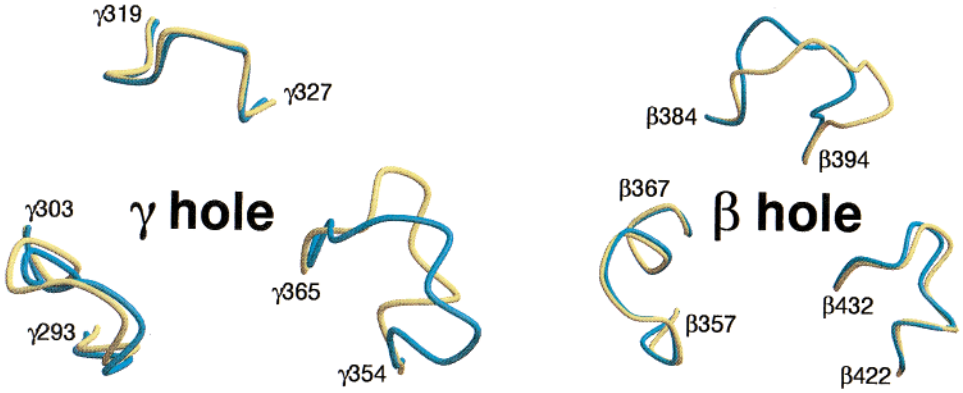

FIGURE 5: Superposition of Cα backbone traces for the loops at the entryways of *γ*-chain (left) and *β*-chain holes (right). Each hole has two loops in common and a third that is changed. Yellow = lamprey; blue = human.

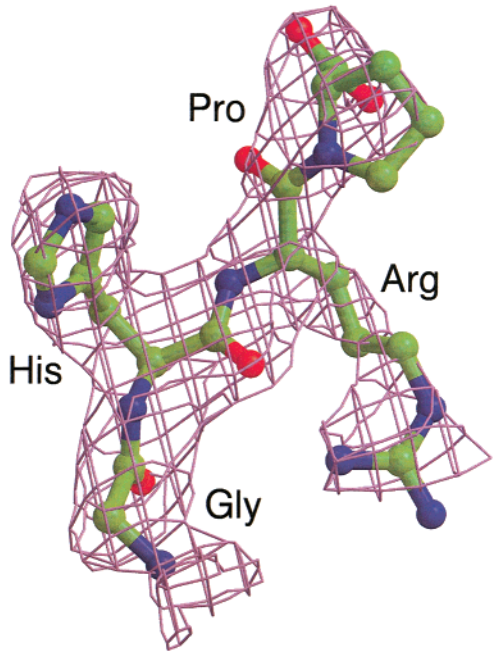

FIGURE 6: Electron density omit map showing peptide ligand GHRPam in the β-chain binding site. The density was calculated from the $|F_o| - |F_c|$ coefficients and phases from the refined model and contoured at 1.5σ. The ligand was not included in the calculation.

are located at residues γ397−γ399 (lamprey numbering) and the putative lysine donor is at residue γ401.

Calcium Binding Sites. Electron density corresponding to calcium atoms is prominent in the homologous primary binding sites on the γ and β chains (γ316−γ322 and β379−β385, respectively). No density was evident, however, in the region between the βC domain and the coiled coil where secondarily bound calcium has been observed in human fragments D (*22*). The situation in another secondary binding site, γ294−γ301, which has a bound calcium in human fragment D only when GHRPam occupies the A hole, was not so clear. The diffuse density in this region of the lamprey structure suggests partial occupancy by a calcium atom, in line with the likelihood that GHRPam may also be partially bound.

Carbohydrate. Lamprey fragment D has asparagine-linked carbohydrate at two different positions: one corresponding to a cluster that occurs in other vertebrate fibrinogens at residue β364 (human numbering; the corresponding lamprey residue is β384) and an additional cluster at γ-chain residue Asnγ203. The first of these clusters is especially well resolved in the DEF and JKL molecules, to the point where the split in the biantennary cluster is readily evident; it was possible to build in seven sugar residues. The clarity of the electron density is at least partly due to the cluster being immobilized by its participation in the crystal packing. As in the human molecule, this cluster sits adjacent to the β-chain hole and may influence access to it. In the case of the second carbohydrate cluster, at Asnγ203, three sugar residues were easily modeled into each of the molecules.

DISCUSSION

The fact that lamprey fibrinogen is readily converted to fibrin by the exclusive release of the fibrinopeptides B (*2*, *4*) provides a unique tool for studying the role of the B knobs.

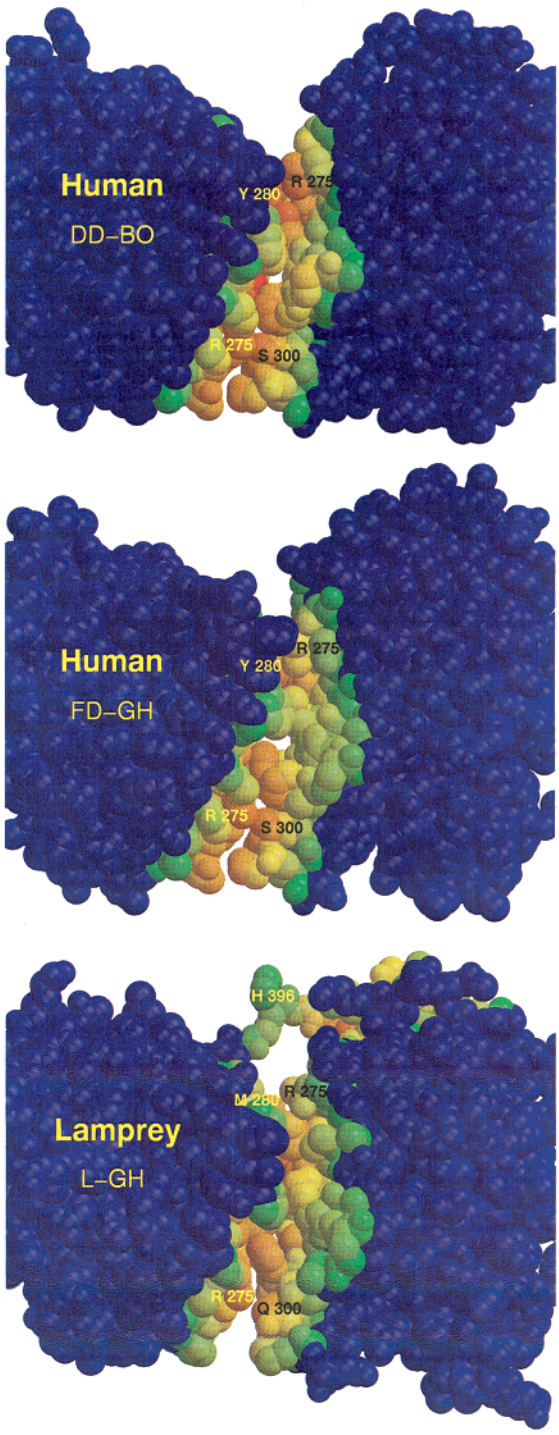

FIGURE 7: Comparison of D:D interfaces for lamprey and two human preparations. Residues are colored according to their distances from nearest residues on the opposite molecule. Argγ275 and its nearest partner are labeled in all molecules. Top, human DDBO (1FZC); middle, human fDGH (1FZC); bottom, lamprey (1LWU). Note the position of Hisγ396 (human numbering) near the carboxyl terminus of lamprey γ chain.

That the reaction is strongly inhibited by GPRPam (the A knob) seems at first glance paradoxical. Moreover, even though the new amino-terminal sequence revealed by the cleavage is Gly-Val-Arg, the corresponding Gly-Val-Arg-Pro (GVRP) synthetic peptide is only a very weak inhibitor of the process (*5*). That the synthetic peptide GPRP is a strong inhibitor, associating more tightly with lamprey fibrinogen than it does with mammalian ones (*5*), suggests

that it is the γ-chain hole that is being blocked, preventing its interaction with the exposed B knobs. Consistent with this interpretation, $\gamma-\gamma$ cross-linking occurs in the usual fashion when activated factor XIII is present, even though only the lamprey fibrinopeptides B are released (*3*), indicating that end-to-end polymerization is occurring normally.

One interpretation of these observations would have the β-chain knobs somehow find the holes normally occupied by the α-chain knobs; an alternative explanation is that the exclusive interaction of B knobs with β-chain holes can result in the same kind of initial association caused by A knobs fitting into the γ-chain holes. The latter scenario would be consistent with a recent model for B-knob involvement (*21*), but it implies that inhibition by GPRP is due to its binding at the β-chain hole, an interaction that does not seem to occur in human fragment D (see below). We hope to resolve the matter by determining the structure of lamprey fragment D complexed with GPRPam.

Knobs and Holes. Synthetic peptides corresponding to the knobs involved in fibrin formation have proved to have a great influence on the mode of crystallization of various fragments D and double-D (*22*). When fragment double-D from human fibrin is cocrystallized with the synthetic A knob, GPRPam, the peptide is bound exclusively in the γ-chain hole, no density at all being found in the β-chain hole (*23*). The certainty of the observation is attested to by the fact that the side chains of β397 and β398 are directed away from the β-chain pocket. When human double-D is cocrystallized with both A and B knobs, each knob finds its own hole, the A knob residing exclusively in the γ chain and the B in the β chain. Even at 2.3 Å resolution, however, it was not possible to determine the subtle structural differences in the two homologous systems that allow this discrimination (*20*). Indeed, the two ligands adopt exactly the same position in their pockets, even to the extent of a subsidiary water molecule involved in the binding.

In the case of human fragment D complexed with only GHRPam, however, the peptide was found in both the β- and γ-chain holes (*23*). In the lamprey complex reported here the peptide is only clear in the β-chain hole; its apparent absence from the γ-chain hole may be due to differences in the entryway loops (Figure 5).

It is unclear why it is so much easier to crystallize fragments D (and double-D) with GHRPam than is the case with GPRPam. One factor may be the conformational change that occurs in the β chain upon binding the peptide, the side chains of Gluβ397 and Aspβ398 moving from a position near the coiled coil to form the final leg of the β-chain binding pocket (*22*). It may be, also, that binding the positively charged ligand alters the charge situation sufficiently in this region of the molecule to favor lateral growth.

The lamprey is the second instance of GHRPam binding to a β-chain hole even though the Gly-His-Arg- sequence does not occur naturally in the native protein. In chicken fibrinogen the corresponding B knob begins with the sequence Ala-His-Arg-Pro. Nonetheless, GHRPam was readily observable in the β-chain pocket of crystals of native chicken fibrinogen crystallized in its presence (*25*).

Carboxyl Terminus of the γ Chain. The carboxyl-terminal segment of the γ chain is one of the most elusive structural features in fibrinogen. It is a region of great physiological importance in that it is the primary site for factor XIII cross-linking and, at least in mammalian fibrinogens, because this part of the molecule is known to bind to platelets and other cells (*26*). The flexibility of the region was first demonstrated by Yee et al. (*27*), who observed multiple conformations in a crystallized recombinant γC domain, including two different forms in the same crystal, neither of which could be observed to the very end of the chain. Experiments with carrier-driven crystallization of the γ-chain carboxyl-terminal 14 residues from human fibrinogen fused with lysozyme (*28*) and glutathione *S*-transferase (*29*) have revealed a Z-shaped structure that overlaps, in part, one of the forms from the recombinant γ chain.

In previous studies of fragments D and double-D, however, the electron density in this region has been too diffuse for modeling. This was especially disappointing in the cases of double-D, where it had been thought the important ϵ-amino-(γ-glutamyl)lysine cross-links between molecules would be visualized. The lamprey fragment D structure has provided the best picture yet for a naturally occurring arrangement between abutting D domains, different conformations existing on the two sides of the abutment. Although this may be attributable to the particular nature of the crystal packing, it offers hope that crystals of factor XIII cross-linked double-D from lamprey fibrin might reveal the cross-links themselves, something that has not been possible heretofore. The basis for this optimizm stems from the fact that, in the case of the human fragments, the crystals for the fragment D−GHRPam complex were isomorphous with those for the cross-linked double-D−GHRPam complex (*22*).

Carbohydrate Clusters. Asparagine-linked carbohydrate is generally regarded as a barrier to crystallization because of its mobile nature. Nonetheless, even though lamprey fragment D contains an additional cluster relative to the corresponding fragments from other vertebrates, crystals were obtained. One of the carbohydrate clusters participates in the crystal packing and was surprisingly well resolved.

It should be noted that the second carbohydrate cluster (Asnγ203) occurs exactly at the same position as where some (homologous) fibrinogen-related proteins have putative carbohydrate attachments (*30*), including a T-cell cytotoxic protein from mouse (*31*) and human (*32*). A similar cluster exists only two residue positions away in several other homologous proteins, including the αEC domain that occurs in a minor alternative form of fibrinogen (*33*, *34*). In this latter case, a crystal structure of a recombinant domain at 2.1 Å resolution revealed four sugar residues (*35*).

In summary, the structure of vertebrate fibrinogen—as typified by its fragment D portions—has been highly conserved over the last 450 million years. The inner portions of the ligand binding sites in the βC and γC regions of the molecule are well preserved, but in each case one of the entryway loops differs and may influence the ability to discriminate between knobs.

Other features of the molecule are also well conserved. For example, the putative stimulator of t-PA, a site on the α chain (residues α151−α158, human numbering) (*36*), has virtually the same sequence in lamprey as occurs in mammals and is wholly inaccessible to solvent in fragment D, just as is the case in mammalian fibrinogens. In a sense, it is remarkable that so much about lamprey fibrinogen is so similar to mammalian counterparts, especially when it is

considered that no earlier diverging organisms have been identified that have a thrombin-clottable fibinogen.

ACKNOWLEDGMENT

We are grateful to Dr. Andrew Laudano for providing lamprey blood plasma. We also thank the staff at the National Light Source, Brookhaven National Laboratory, for their cooperation during our visit.

REFERENCES

1. Doolittle, R. F., Oncley, J. L., and Surgenor, D. M. (1962) *J. Biol. Chem. 237*, 3123−3127.
2. Doolittle, R. F. (1965) *Biochem. J. 94*, 735−741.
3. Doolittle, R. F. (1991) in *Fibrinogen, Thrombosis, Coagulation and Fibrinolysis* (Liu, C. Y., and Chien, S., Eds.) pp 25−37, Plenum Press, New York.
4. Doolittle, R. F., and Cottrell, B. A. (1976) *Biochim. Biophys. Acta 453*, 426−438.
5. Laudano, A. P., and Doolittle, R. F. (1980) *Biochemistry 19*, 1013−1019.
6. Doolittle, R. F., Schubert, D., and Schwartz, S. A. (1968) *Arch. Biochem. Biophys. 118*, 456−467.
7. Kuyas, C., Haeberli, A., Walder, P., and Straub, P. W. (1990) *Thromb. Haemostasis 63*, 439−444.
8. Yamazumi, K., and Doolittle, R. F. (1992) *Proc. Natl. Acad. Sci. U.S.A. 89*, 2893−2896.
9. Otwinowski, Z., and Minor, W. (1997) *Methods Enzymol. 276*, 307−326.
10. Navaza, J. (1994) *Acta Crystallogr. A50*, 157−163.
11. Collaborative Computing Project Number 4 (1994) *Acta Crystallogr. D50*, 760−763.
12. Jones, T. A., Zou, J.-Y., Cowan, S. W., and Kjeldgaard, M. (1991) *Acta Crystallogr. A47*, 110−119.
13. Brunger, A. T., Adams, P. D., Clore, G. M., DeLano, W. L., Gros, P., Grosse-Kunstleve, R. W., Jiang, J.-S., Kuszewski, J., Nilges, M., Pannu, N. S., Read, R. J., Rice, L. M., Simonson, T., and Warren, G. L. (1998) *Acta Crystallogr. D54*, 905−921.
14. Brunger, A. T. (1992) *Nature 355*, 472−475.
15. McRee, D. E. (1992) *J. Mol. Graphics 10*, 44−46.
16. Kraulis, P. J. (1991) *J. Appl. Crystallogr. 24*, 946−950.
17. Bacon, D. J., and Anderson, W. F. (1988) *J. Mol. Graphics 6*, 219−220.
18. Merritt, E. A., and Murphy, M. E. P. (1994) *Acta Crystallogr. D50*, 869−873.
19. Doolittle, R. F., Watt, K. W. K., Cottrell, B. A., Strong, D. D., and Riley, M. (1979) *Nature 280*, 464−468.
20. Everse, S. J., Spraggon, G., Veerapandian, L., Riley, M., and Doolittle, R. F. (1998) *Biochemistry 37*, 8637−8642.
21. Read, R. J. (1986) *Acta Crystallogr. A42*, 140−149.
22. Everse, S. J., Spraggon, G., Veerapandian, L., Riley, M., and Doolittle, R. F. (1999) *Biochemistry 38*, 2941−2946.
23. Spraggon, G., Everse, S. J., and Doolittle, R. F. (1997) *Nature 389*, 455−462.
24. Brown, J. H., Volkmann, N., Jun, G., Henschen, A. H., and Cohen, C. (2000) *Proc. Natl. Acad. Sci, U.S.A. 97*, 85−90.
25. Yang, Z., Kollman, J. M., Pandi, L., and Doolittle, R. F. (2001) *Biochemistry 40*, 12515−12523.
26. Hawiger, J. (1995) *Semin. Hematol. 32*, 99−109.
27. Yee, V. C., Pratt, K. P., Cote, H. C., LeTrong, I., Chung, D. W., Davie, E. W., Stenkamp, R. E., and Teller, D. C. (1997) *Structure 5*, 125−138.
28. Donahue, J. P., Patel, H., Anderson, W. F., and Hawiger, J. (1994) *Proc. Natl. Acad. Sci. U.S.A. 91*, 12178−12182.
29. Ware, S., Donahue, J. P., Hawiger, J. and Anderson, W. F. (1999) *Protein Sci. 8*, 2663−2671.
30. Doolittle, R. F. (1992) *Protein Sci. 1*, 1563−1577.
31. Koyama, T., Hall, L. R., Haser, W. G., Tonegawa, S., and Saito, H. (1987) *Proc. Natl. Acad. Sci. U.S.A. 84*, 1069−1613.
32. Ruegg, C., and Pytela, R. (1995) *Gene 160*, 257−262.
33. Fu, Y., Cao, Y., Hertzberg, K. M., and Grieninger, G. (1995) *Genomics 30*, 71−76.
34. Pan, Y., and Doolittle, R. F. (1992) *Proc. Natl. Acad. Sci. U.S.A. 89*, 2066−2070.
35. Spraggon, G., Applegate, D., Everse, S. J., Zhang, J.-Z., Veerapandian, L., Redman, C., Doolittle, R. F., and Grieninger (1998) *Proc. Natl. Acad. Sci. U.S.A. 95*, 9099−9104.
36. Schielen, W. J. G., Voskuilen, M., Tesser, G. J., and Nieuwenhuizen, W. (1989) *Proc. Natl. Acad. Sci. U.S.A. 86*, 8941−8954.

BI020299T